Effects of synthesis parameters on electrical conductivity and microstructural development of fine zirconia powders

D. M. ÁVILA, E. N. S. MUCCILLO
Instituto de Pesquisas Energéticas e Nucleares, Comissão Nacional de Energia Nuclear, CP 11049, Pinheiros, S Paulo, 05422-970 SP, Brazil

Zirconia ceramic powders have been prepared by a variety of methods. The methods based on solution chemistry have been recognized as the most used due to their simplicity and cost-to-benefit ratio [1]. Besides phase composition, one of the most studied characteristic of the fine powders obtained by chemical methods has been the agglomeration state [2–6]. Agglomeration is a common and deleterious characteristic of powders prepared by wet chemical methods. It influences densification and grain growth rate thereby affecting microstructure development [7]. In this context, two strategies have been put forward: to avoid the development of "hard agglomerates", and to separate once they are formed. Generally, the former is accomplished by introducing a special step in the processing sequence before calcination; washing and drying steps have been used in this case. Washing with organic liquids is usually employed for this purpose, giving rise to "soft" and "loose" ceramic powders [8–11]. In the case of zirconia-based materials, high sintered densities have been obtained.

This letter describes the electrical behaviour and the microstructural development of sintered pellets prepared with fine zirconia powders obtained by the precipitation technique under different pH, precipitation temperatures, and washing media. To prepare the pellets, magnesium oxide was added as a stabilizing agent. The main purpose was to investigate how these processing variables can influence the electrical conductivity and the microstructure of the sintered ceramic material.

Zirconia powders were prepared by the precipitation technique. A 0.6 M $ZrOCl_2 \cdot 8H_2O$ (99.5% Riedel de Häen) aqueous solution was added dropwise to a precipitant under vigorous stirring. The resulting gelatinous precipitate was washed and collected by vacuum filtration several times. Samples were dried at 110 8C for 24 h and calcined at 600 8C for 30 min in air. Further details on powder preparation and analyses were given earlier [12]. Specific synthesis conditions for each sample are listed in Table I. Magnesium oxide (Carlo Erba, P.A.) was added by wet mixing to each zirconia sample in order to give a fixed 8 mol % concentration. Pellets of 12 mm diameter and 2 mm thickness were prepared by uniaxial pressing at 196 MPa and sintered at 1450 8C for 4 h in air.

Apparent density was determined by the hydrostatic method. X-ray diffraction patterns were obtained with a Rigaku diffractometer using a Ni filtered $CuK_{Æ}$ radiation. The volume fraction of each phase was estimated from the ratio of the corresponding 100% peak intensities [13]. Fractured surfaces were observed in a JXA 6400 Jeol scanning electron microscopy. Two-probe d.c. resistivity measurements between 400 8C and 700 8C were carried out on an alumina sample chamber with Pt leads and a Pt/Pt-10% Rh thermocouple to monitor sample temperature, all inserted in a temperature-controlled tubular furnace. A 616 Keithley digital electrometer was used. Platinum electrodes were applied by sputtering. Impedance measurements in the 5 Hz to 13 MHz frequency range were performed on the same specimens with an HP 4192A impedance analyser. Data were collected during heating and cooling cycles between 300 8C and 500 8C. Silver electrodes were applied by painting and subsequent baking at 500 8C.

Values of apparent density, diametral shrinkage, volume fraction of monoclinic (V_m) phase, and average grain size for sintered specimens are given in Table II. Assuming a theoretical density (TD) of 5.83 mg m^{-3} for this composition [14], and 5.56 mg m^{-3} for the m-phase (sample 6), all sintered specimens reached densities between 90% and 96%

TABLE I Specific synthesis parameters used in the preparation of fine zirconia powders

Specimen	pH	Temperature[a] (8C)	Washing media[b]
1	6	RT	w + e
2	10–11	RT	w + e
3	13	RT	w + e
4	13	40	w + e
5	10–11	RT	a + e
6	10–11	RT	w + e + ATA

[a]RT, room temperature; [b]w, water; e, ethanol; a, 0.2 N NH_4OH solution, and ATA, acetone-toulene-acetone.

TABLE II Values of hydrostatic density (d_h), diametral shrinkage (DS), volume fraction of monoclinic phase (V_m), and average grain size (D) for sintered specimens

Specimen	d_h (mg m^{-3})	DS (%)	V_m (%)	D (ìm)
1	5.63	22.3	50	1.2
2	5.23	21.7	45	1.0
3	5.53	20.0	75	1.5
4	5.62	23.3	55	0.9
5	5.40	27.3	37	0.8
6	5.16	31.2	100	4.0

0261-8028 © *1997 Chapman & Hall*

TD. Higher shrinkage is observed when zirconia powders are washed with a diluted ammonia solution or following the ATA (acetone-toluene-acetone) sequence. This is a consequence of better water removal from the precipitated gel avoiding formation of hard agglomerates. Even after calcination, powders 5 and 6 presented a "loose aspect" and higher specific surface area values [12] compared with other specimens. Considering powders obtained by precipitation at different pH, the fraction of monoclinic phase in sintered material is considerably higher for higher pH (specimen 3), although this specimen presented only the tetragonal phase after calcination. The high monoclinic content in the sintered material may be attributed to the average crystallite size being about twice that of the same phase in specimens 1 and 2 [12]. Concerning the precipitation temperature (specimens 3 and 5), the m-phase content is higher for room temperature experiments. These results are also related to the growth of the crystallite size during sintering beyond the threshold value for the tetragonal-monoclinic phase transformation. The effect produced by the washing media (specimens 2, 5 and 6) is a remarkable increase in the monoclinic phase content for the specimen treated following the ATA sequence.

Scanning electron micrographs of fractured surfaces are shown in Fig. 1. Specimens washed with

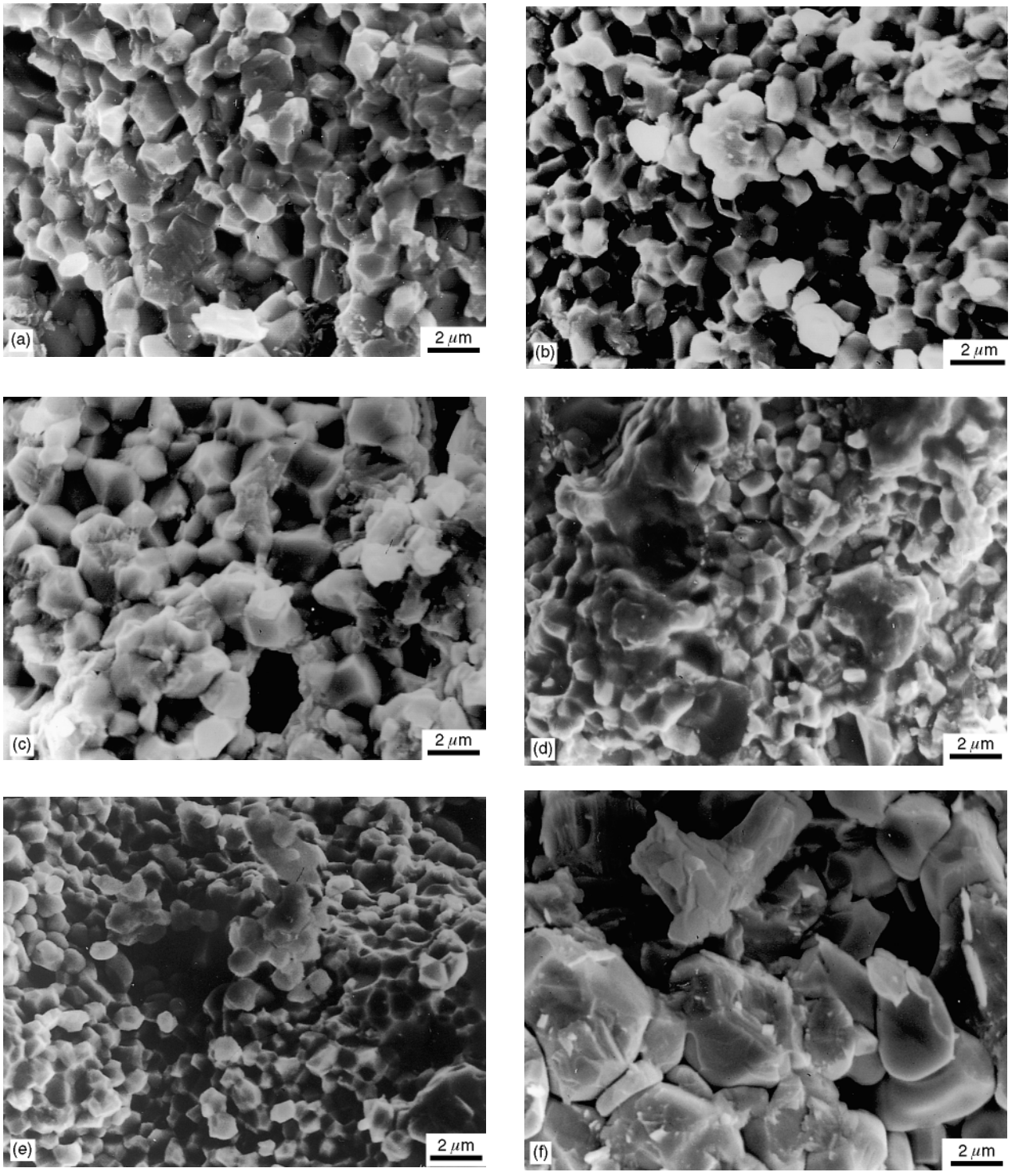

Figure 1 Scanning electron micrographs of fractured sintered specimens: (a) 1; (b) 2; (c) 3; (d) 4; (e) 5 and (f) 6.

water and ethanol (1, 2, 3, and 4; a, b, c, and d, respectively) exhibit angular grains with uniform grain size distribution, and few large (cubic) grains. Grain size is larger in the case of precipitation at pH 13 at room temperature (c). Specimens treated with ammonia (e) or the ATA sequence (f) have more rounded grains. The former present the smallest grains along with few large grains, while the latter exhibit coarse and irregularly shaped grains, as shown in Fig. 2 with a higher magnification. Estimated values of average grain sizes are given in Table II.

More than one process usually contributes to mass transport during sintering. It has been shown [15, 16] that vapour transport is enhanced by either the ambient atmosphere or the presence of a vapour producing-phase within the powder compact. If this mechanism predominates in the early stages of sintering, reduced shrinkage and grain coarsening are expected. In the final stage of sintering, however, densification is not inhibited. These results on apparent density and electron microscopy suggest that vapour transport plays the major role in the final stage of sintering of the ATA-derived powder.

Fig. 3 shows impedance diagrams of specimens 4 and 5 measured at 460 8C. These diagrams are typical of Mg-partially stabilized zirconia ceramics consisting of three semicircles attributed to grains (high frequency), grain boundaries (low frequency), and to the blocking of charge carriers by the monoclinic grains and/or pores (intermediary frequency) [17]. These semicircles are partially overlapped making resolution of the impedance diagrams not straightforward.

Arrhenius plots of electrical resistivity of specimens prepared under different pH, precipitation temperatures, and washing media are shown in Fig 4a, b, and c, respectively. The main observed difference is related to specimens obtained after

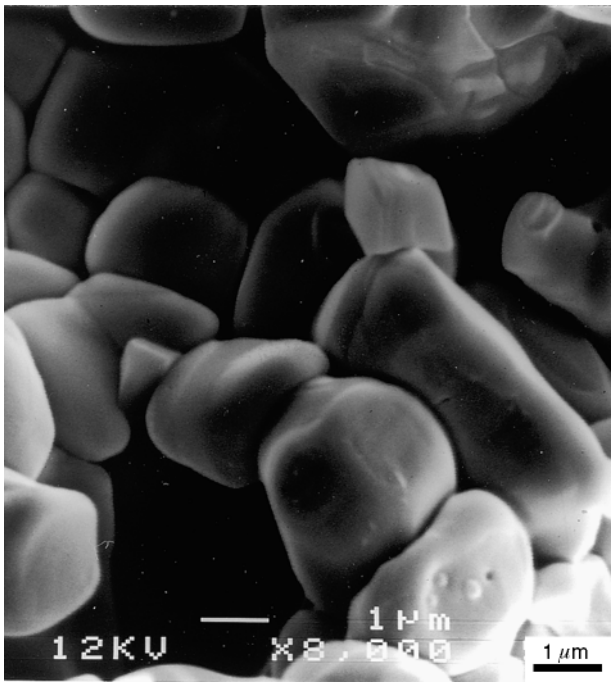

Figure 2 Fractured surface of specimen 6.

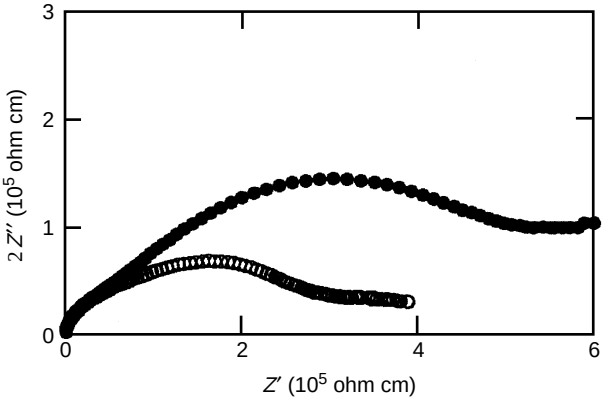

Figure 3 Impedance diagrams of specimens 4, (○) and 5, (●) at 460 8C.

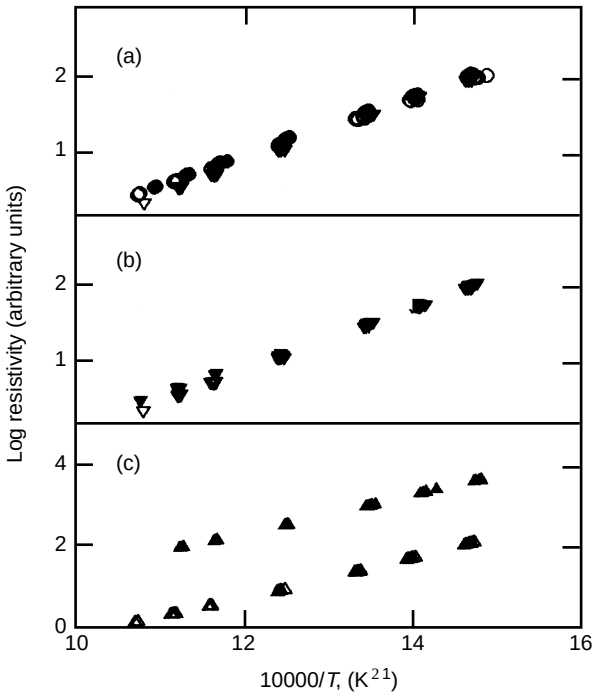

Figure 4 Arrhenius resistivity plots for different synthesis parameters: (a) pH, ○ 1, ● 2, ▽ 3; (b) precipitation temperature, ▽ 3, ▼ 4 and (c) washing media, △ 5, ▲ 6.

different washing conditions. Specimens treated following the ATA sequence exhibit values of electrical resistivity two orders of magnitude higher than for other specimens. This was expected because the monoclinic phase is more resistive than the tetragonal and cubic phases. The activation energy value for specimens 1 to 4 is approximately 0.80 eV, while that for specimens 5 and 6 is 0.96 eV. The activation energy for the conduction process in zirconia-magnesia solid solutions is a composition-dependent parameter [17]. For specimen 5, the increase in activation energy can be attributed to enhanced solid solution formation as a consequence of a high degree of agglomerates dispersion after the ammonia treatment. On the other hand, even though powder agglomerates of specimen 6 are highly dispersed, a solid solution is not easily attained, as shown by X-ray diffractometry. In this case, the calculated activation energy value is between those of the m-phase in "pure" (1.22 eV) and Mg-doped (0.70 eV) zirconias [17].

Our results show that many structural differences observed in calcined powders prepared from precipitation are lost during the sintering process, resulting in ceramic bodies with very similar electrical properties, except for minor differences in the final microstructure. The main conclusion is that the washing media play the major role in both microstructural development and electrical resistivity in sintered zirconia ceramics.

Acknowledgements

The authors acknowledge the technical assistance of C. V. Morais, M. M. Serna, R. M. R. Pasotti and Y. V. França.

References

1. D. W. JOHNSON, JR., in "Ceramic Powder Science", Advances in Ceramics, Vol. 21, edited by G. L. Messing, K. S. Mazdiyasni, J. W. McCauley, and R. A. Haber (The American Ceramic Society, Westerville, Ohio, 1987) p. 3–19.
2. M. A. C. G. van de GRAAF, K. KEIZER and A. J. BURGGRAAF, *Sci. Ceram.* **10** (1979) 83.
3. F. F. LANGE, *J. Am. Ceram. Soc.* **67** (1984) 83.
4. J.-M. WU and C.-H. WU, *J. Mater. Sci.* **23** (1988) 3290.
5. J.-L. SHI, J.-H. GAO, Z.-X. LIN and T. S. YEN, *J. Am. Ceram. Soc.* **74** (1991) 994.
6. J.-L. SHI, J.-H. GAO, Z.-X. LIN and D.-S. YAN, *J. Mater. Sci.* **28** (1993) 342.
7. J. W. HALLORAN, in "Forming of Ceramics", Advances in Ceramics, Vol. 9, edited by J. A. Mangels and G. L. Messing (The American Ceramic Society, Columbus, Ohio, 1984) p. 67–75.
8. S. L. DOLE, R. W. SCHEIDECKER, L. E. SHIERS, M. F. BERARD and O. HUNTER, JR., *Mater. Sci. Eng.* **32** (1978) 277.
9. K. HABERKO, *Ceram. Int.* **5** (1979) 148.
10. M. S. KALISZEWSKI and A. H. HEUER, *J. Am. Ceram. Soc.* **73** (1990) 1504.
11. P. D. L. MERCERA, J. G. van OMMEN, E. B. M. DOESBURG, A. J. BURGGRAAF and J. R. H. ROSS, *J. Mater. Sci.* **27** (1992) 4890.
12. D. M. ÁVILA and E. N. S. MUCCILLO, *Thermochim. Acta* **256** (1995) 321.
13. D. L. PORTER and A. H. HEUER, *J. Am. Ceram. Soc.* **62** (1979) 298.
14. R. STEVENS, in "An introduction to zirconia", No. 113 (Magnesium Elektron Ltd, Twickenham, UK, 1986).
15. M. J. READEY and D. W. READEY, *J. Am. Ceram. Soc.* **69** (1986) 580.
16. D. W. READEY, in "Sintering of Advanced Ceramics", Ceramic Transactions Vol. 7, edited by C. A. Handwerker, J. E. Blendell, and W. A. Kaysser (The American Ceramic Society, Westerville, Ohio, 1990) p. 86–110.
17. E. N. S. MUCCILLO and M. KLEITZ, *J. Eur. Ceram. Soc.* **16** (1996) 453.

Received 5 March 1996
and accepted 7 January 1997